Progress In Electromagnetics Research C, Vol. 90, 15–28, 2019

Design and Manufacturing of a Novel Compact 2.4 GHz LPF Using a DGS-DMS Combination and Quasi Octagonal Resonators for Radar and GPS Applications

Ahmed Boutejdar[1, *], Mouloud Challal[2], Sudipta Das[3], and Soumia El Hani[4]

Abstract—In this paper, a new compact microstrip low-pass filter (LPF) with ultra-wide stopband characteristics is presented. The combinations of DGS-DMS along with quasi octagonal resonators are employed in the design of the proposed filter to achieve compact size and ultra-wide stopband suppression level. The proposed filter has been designed, simulated, optimized and tested. The design procedure is validated using the commercial full-wave EM MoM simulator Microwave Office. Simulated as well as measured results of low-pass filter exhibit sharp roll-off (ξ) of 19 dB/GHz and creating transmission zero at around 7.8 GHz with attenuation level -54 dB. The measurement results show good agreement with the simulations. The cutoff frequency of the proposed low-pass filter is 2.4 GHz with the insertion loss less than 0.3 dB. The ultra wide stopband with over 20 dB attenuation extended from 3.42 GHz to 12 GHz. The spurious passband suppression up to six harmonics ($5fc$) is achieved for the proposed design. The addition of two parasitics DGS elements in the ground plane leads to suppression of the undesired harmonics und thus to improve the stopband. The size of the whole structure is less as ($0.44\lambda_g \times 0.26\lambda_g$) with $\lambda_g = 68$ mm. The proposed filter is useful for microwave L band, GPS system, and RADAR applications.

1. INTRODUCTION

The rapid growth of modern wireless communication has increased the demand for compact, low cost and high performance components. Microstrip filter is one of the vital components in modern wireless communication systems. Microstrip low-pass filter with ultra-wide stopband is also a very crucial component in wireless communication systems to suppress unwanted high frequency harmonics. The modern wireless communication demands compact filters with low insertion loss and high return loss in the passband and high rejection in the stopband. To meet requirements, researchers have reported various design approaches in literature for the design of low-pass filters with wide rejection band [1, 2]. In [2], a quasi-elliptic filter uses an interdigital structure between the symmetric rectangular couple capacitors which reduces the size of the filter. A compact LPF using embedded band-stop structure is proposed in [3]. In [4], another low-pass filter with sharp roll-off is proposed using cascaded multiple patch resonators, but only second harmonic suppression could be reached. Low-pass filters with microstrip coupled line hairpin units are demonstrated in [5, 6] to achieve expanded stopband, but these filters suffer from low roll-off rate and high return loss in the stopband. A compact low-pass filter using tri-section SIR is proposed to achieve wide rejection band [7]. A compact low-pass filter using semi-circular stepped impedance resonators and open stubs is proposed in [8]. Another design technique of a low-pass filter to get wide stopband is proposed in [9] by employing a G-shaped DMS but at the

Received 21 September 2018, Accepted 8 December 2018, Scheduled 10 January 2019

* Corresponding author: Ahmed Boutejdar (boutejdar69@gmail.com).

[1] German Research Foundation (DFG), Braunschweig-Bonn, Germany. [2] University Boumerdes, Institute of Electrical and Electronic Engineering, Boumerdes, Algeria. [3] Department of Electronics and Communication Engineering, IMPS College of Engineering, W.B, India. [4] Mohammed V University in Rabat, ENSET, Rabat, Morocco.

cost of large physical size. In recent years, defective ground structures (DGS) have been widely used for LPF designs [10, 11]. In [11], two quasi elliptic low-pass filters with wideband reject characteristics are designed using interdigital defected ground structure. A novel combination of elliptic shaped DGS and H-shaped open stubs is used for the design of a low-pass filter, but the stopband bandwidth of only 4.83 GHz is achieved [12].

The topology of slit-loaded tapered microstrip resonator cell has been employed in the design of low-pass filter to achieve sharp cutoff frequency, but the stopband suppression level is only 10 dB, and large layout area is also required for the design of this filter [13]. The combination of quasi-Yagi DGS resonator and multilayer technique is used by Boutejdar and Ali to improve the compactness of LPF [14]. A low-pass filter based on combination of defected ground structure (DGS), defected microstrip structure (DMS), and compensated microstrip capacitors is proposed in [15]. In [16], a compact microstrip low-pass filter has been reported using a coupled DGS and a compensated microstrip line to achieve high rejection and wide stopband. A simple low-pass filter using a three cascaded U-shaped defected ground structure and compensated microstrip line is reported in [17]. In [18], the performance of microstrip low-pass filter has been investigated by employing a coupled C-shaped defected ground structure. The effect of periodic dumbbell slots in the ground plane has been investigated for achieving sharp transition band in low-pass filter [19–23]. An LPF is designed using double equilateral U-shaped defected ground structure for wide rejection band [24, 25]. In order to improve the transition domain and the rejectband of low-pass filter, other researchers have been developed, and another method is called metamaterial LPF based on the combination of microstrip resonator and defected ground structure including stubs [26].

In this paper, a new compact microstrip low-pass filter using coupled DMS, DGS and quasi-octagonal resonators is reported. Several studies have been performed on the influence of the geometric modification of this filter on its characteristics. The combination of triangular head DGS-DMS along with two quasi octagonal resonators is used to improve the compactness of the proposed filter due to slow wave effect and suppress the high frequency harmonics in order to achieve a wide stopband. A new very compact low-pass filtering topology is designed and optimized. Finally, the proposed low-pass filter has been fabricated and measured. The measured results show excellent agreement with the simulated ones. Several improvements are obtained for the response of LPF due to the proposed design topology such as (i) suppression of higher frequency harmonics up to $5f_c$, (ii) ultra-wideband reject response, (iii) improvement in the stop and pass band characteristics, (iv) good transition sharpness with low insertion loss in the passband.

2. CHARACTERISTICS OF THE OCTAGONAL MICROSTRIP RESONATOR

Figures 1 and 2 show the simple octagonal and the quasi octagonal microstrip resonators, respectively. This topology is placed on the top layer, and it is excited by 50 Ω feed line. The octagonal resonator is coupled to metallic ground plane through a dielectric substrate with $\varepsilon_r = 3.38$ and thickness $h = 0.813$ mm. The investigated resonator consists of two octagonal heads, which are connected with a slight metallic channel. The octagonal patch corresponds to an equivalent capacitance, and the thin metallic channel corresponds to an equivalent inductance [25]. All the dimensions of the proposed octagonal resonator are depicted in Table 1. The effect of the metallic channel length (h) is examined (see Fig. 3). The width of the connecting thin-line of the proposed resonator cell is made equal to e. The octagonal head area and its dimensions are kept constant as shown in Fig. 1. Based on the information from our own old work [25], it can be deducted that variations of the channel width have only small influence on the center frequency position. On the other hand, the values of stub-length are varied from 2.0 mm to 10 mm, which leads to a variation of cutoff and first attenuation pole frequencies from 3.5 GHz to 1.5 GHz and from 8.8 GHz to 5.2 GHz, respectively. The carried out variations of h show a big influence on the scattering results, thus the position of resonance frequency as well as of cutoff frequency can be simply controlled and adjusted, as shown in Fig. 3.

Fig. 4 shows the equivalent circuit of the quasi octagonal microstrip resonator. The results of EM simulation and equivalent circuit are all shown in Fig. 5, and the good agreement among them demonstrates the validity of equivalent circuit model for the proposed band-stop filter first order. As shown in Fig. 5, the insertion loss from DC to 3 GHz is less than 0.5 dB, and the return loss is less than

Table 1. Dimensions of the DGS, DMS and of octagonal microstrip resonator.

Dimensions of octagonal-resonator	**a**	**b**	**c**	**d**	**e**	**h**	**s**
Values (mm)	2.8	1.8	2.5	2.0	1.0	2.5	3.5
Dimensions of DMS-resonator	**r**	**f**	**n**	**m**	**p**	**w**	
Values (mm)	0.8	1.7	0.5	4.0	0.7	1.9	
Dimensions of DGS-resonator	**v**	**u**	**g**	**t**	**z**		
Values (mm)	8.0	4.5	1.2	2.8	6.0		
Dimensions of parasitic DGS	**x**	**y**	**i**	**q**			
Values (mm)	2.5	2.5	0.8	5.0			

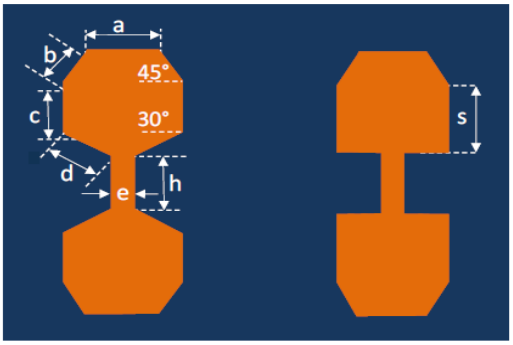

Figure 1. Schematic view of the octagonal-DGS cell. (a) Conventional DGS, (b) improved DGS.

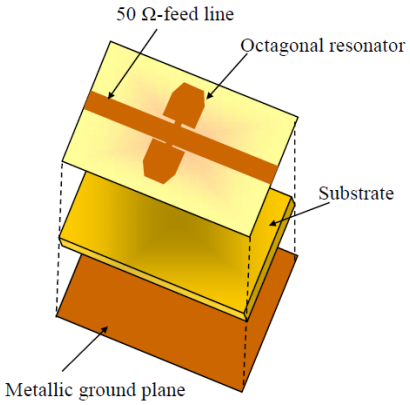

Figure 2. The 3D view of the octagonal resonator on the top layer.

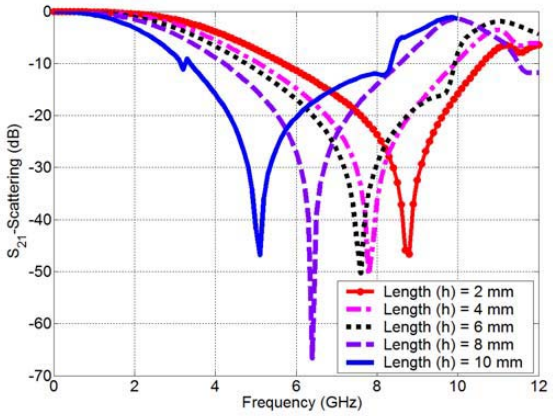

Figure 3. The S_{21} results versus the length h of the octagonal resonator.

-22 dB in the passband. The stopband rejection levels are larger than 20 dB from 4.7 GHz to 6.7 GHz. The size of the proposed band-stop filter is $7 \times 7\,\text{mm}^2$, as can be seen from Fig. 2. The new topology of the quasi octagonal resonator (see Fig. 2) leads to a minimization of radiation loss, especially around the feed line, and thus an improvement of the filter results, which is not the case by using the conventional octagonal resonator (see Fig. 1(a)).

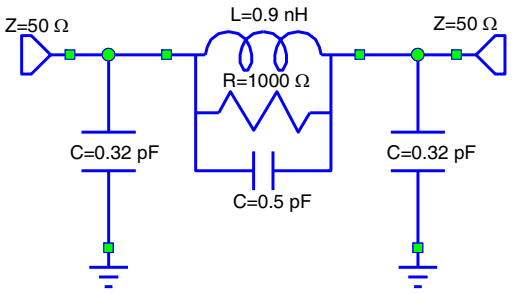

Figure 4. Equivalent circuit model of the proposed octagonal-resonator.

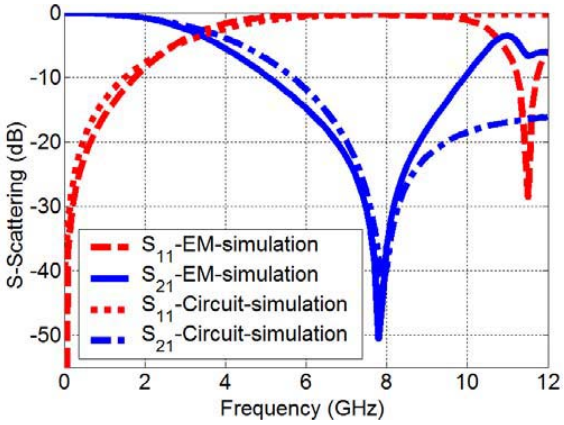

Figure 5. Comparison between the simulation and circuit results of the octagonal-resonator.

The values of circuit parameters R, L, and C can be calculated using result that is matched to the one-pole Butterworth-type low-pass response [25]. Furthermore, radiation effects are more or less neglected. The reactance values of octagonal resonator and filter first order can be expressed as:

$$X_{LC} = \left[\omega_0 C \left(\frac{\omega_0}{\omega} - \frac{\omega}{\omega_0}\right)^{-1}\right] \tag{1}$$

The series inductance (reactance) of one-pole Butterworth low-pass filter can be defined as follows:

$$X_L = \omega L = \omega \left(\frac{g_1 Z_0}{\omega_0}\right) \tag{2}$$

where g_1, Z_0, ω_0, and ω_0 are the prototype value of the Butterworth-type LPF, scaled characteristic impedance, resonant frequency, and cutoff frequency, respectively. By matching the two reactance values in Eqs. (1) and (2), the lumped elements of the equivalent circuit can be derived using the following equations:

$$C = \left(\frac{\omega_c}{2Z_0\left(\omega_0^2 - \omega_c^2\right)}\right) \tag{3}$$

$$L = \left(\frac{1}{\omega_0^2 C}\right) \tag{4}$$

$$R = \frac{2Z_0}{\left(1/\left|S_{11}\left(\omega_0\right)\right|^2 - \left(2Z_0\left(\omega_0 C - 1/\omega_0 L\right)\right)^2\right)^{\frac{1}{2}} - 1} \tag{5}$$

The calculated values of lumped elements C, L, and R are, respectively, 0.31 pF, 1.71 nH, and 762.6 Ω. Fig. 5 shows the comparison between the EM-simulation and circuit results of the proposed octagonal resonator. Their results are in close agreement with each other from DC to $3f_c$.

3. DESIGN OF LOW-PASS FILTER USING TWO OCTAGONAL RESONATORS

A new 2.4 GHz LPF is designed using two cascaded microstrip octagonal resonators, which are placed on the top layer and directly connected with input/output through 50 Ω feed line. Fig. 6 shows the 3D-view of the proposed filter candidat. The two neighbour resonators are electromagnetically coupled. The dimensions of the investigated filter are shown in Table 1, while the coupling distance (z) between two resonators is 6 mm (see Fig. 6). The 50 Ω feed line width is w. The low-pass structure is simulated and optimized by using Microwave Office AWR. The dimensions are calculated using filter theory, Tx-line software and EM simulator. As the scattering results depicted in Fig. 7, the simulation results

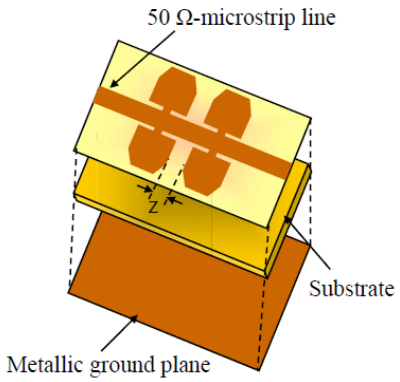

Figure 6. The 3D view of the proposed octagonal LPF.

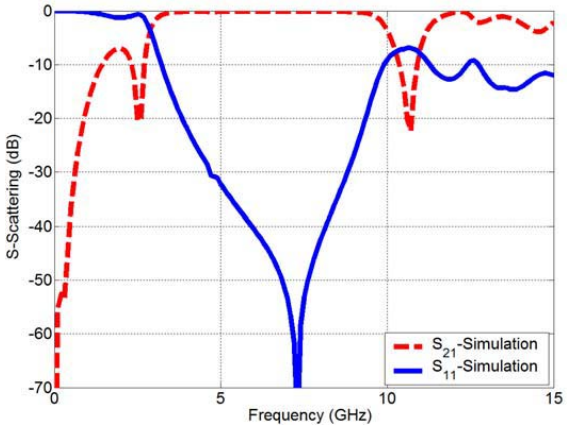

Figure 7. The simulation results of the proposed octagonal LPF.

confirm that at 3-dB cutoff frequency of 2.4 GHz, the low-pass filter exhibits −20 dB stopband that extends from 4.0 to 9.0 GHz. Insertion loss is 0.65 dB in passband, and return loss is equal to −7 dB in the passband. As shown in Fig. 7, the expected responses are not satisfied in the passband; therefore, other techniques will be applied in order to improve these results.

4. CHARACTERISTICS OF THE DMS RESONATOR

A new DMS element, which consists of wide and narrow etched sections, is etched in the feed line. The extremes of this resonator are connected to both SMA connectors through 50 Ω microstrip line. The width $w = 1.9$ mm of the microstrip line is designed to match the characteristic impedance of 50 Ω. The gap between the two DMS arms presents the capacitance, while the rectangular metal area, connected to the arms, corresponds to the inductance (see Fig. 8). Depending on the length of the coupling distance (J-inverter), the scattering responses of DMS cell show several resonance frequencies from 7.5 to 10 GHz (see Fig. 9). The structure has been designed on an RO4003 substrate with the same features as before. As discussed in our old paper [25], the equivalent circuit of the DMS cell acts as a parallel LC resonator. All dimensions of the proposed DMS resonator are depicted in the Table 1. To examine the frequency behaviour of the DMS resonator, a modification of the width of the gap (r) is carried out, while all the other dimensions are kept constant as shown in Fig. 9. The carried out variations on

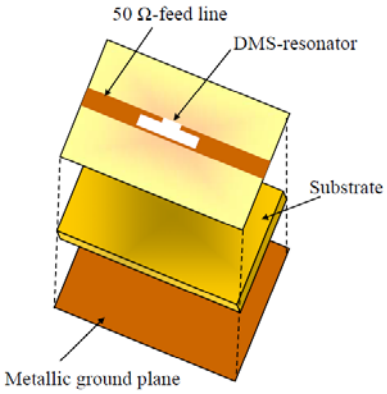

Figure 8. The 3D-view oft he DMS-element.

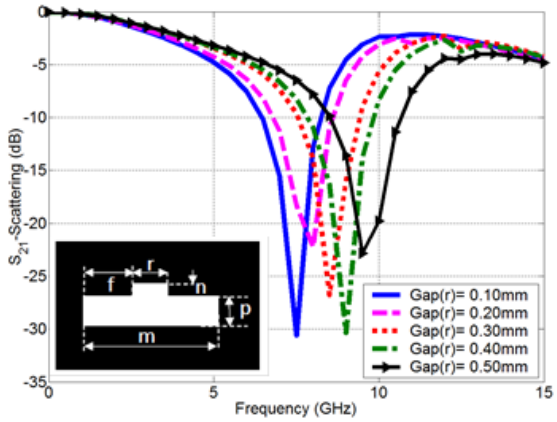

Figure 9. The S_{21} results versus the width of the DMS-gap (r).

r (the value of gap (r) is varied from 0.10 mm to 0.50 mm) show a clear influence on the attenuation pole of the resonator (the first attenuation pole frequency is varied from 7.5 GHz to 9.5 GHz). When the gap increases, the capacitance decreases, and thus the resonance frequency shifts to high frequency range. This characteristic can be used to control the position of the resonance frequency consequently to suppress the undesired harmonics of the filter-topology.

5. DESIGN OF LOW-PASS FILTER USING DMS AND OCTAGONAL RESONATORS

In order to minimise the losses in the passband and thus to improve the features of the 2.4 GHz low-pass filter, two DMS elements have been etched in the 50 Ω feed line. The DMS units are placed at the left and right of the octagonal resonator pair. The design of the DMS-filter is distinguished from the conventional octagonal filter only by the use of DMS units on the top layer. Fig. 10 shows the 3D-view of the proposed DMS low-pass filter. The structure is designed and optimised using AWR simulator.

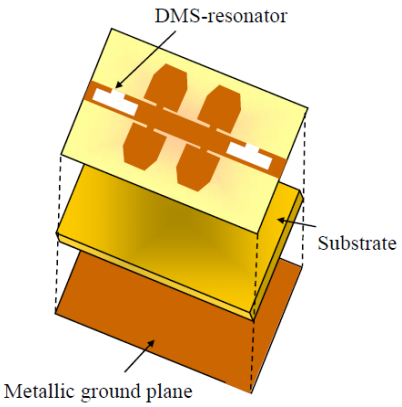

Figure 10. 3D-view oft he DMS-octagonal LPF.

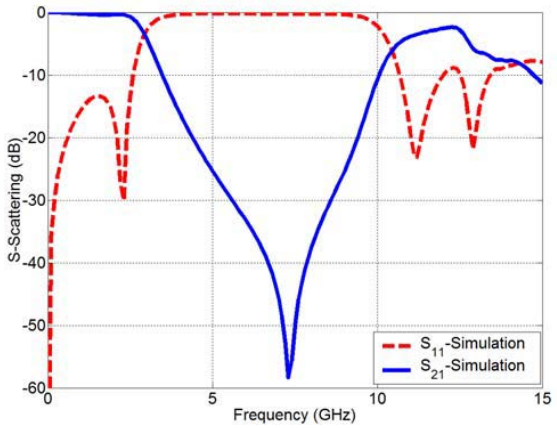

Figure 11. The scattering parameters of the DMS-octagonal LPF.

The simulation results show that the cutoff frequency of designed filter is 2.4 GHz. The structure exhibits a simple design, lower return loss in the passband than filter without DMS and achieves a wide rejection bandwidth with 20 dB attenuation from 4.5 to 9.5 GHz. As shown in Fig. 11, the return loss reaches −13 dB, but this amelioration of filter performance could be further developed; therefore, the DGS technique can be employed in order to further push this improvement.

6. CHARACTERISTICS OF THE DGS RESONATOR

The arrowhead DGS slot is etched in the ground plane (see Fig. 12). The DGS unit is composed of two triangular heads, which are connected to each other through a thin channel (gap). The big area (arrowhead) corresponds to the inductance, while the thin gap to the capacitance. The inductance and capacitance of the DGS slot are computed from the following expressions (1)–(5). As shown in Fig. 13, the pole frequency (f_0) and 3 dB cutoff frequency (f_c) of the resonated DGS slot can be extracted from scattering S-parameter obtained with the help of Microwave Office. In order to demonstrate the effect of the dimensions on the results, a small study is carried out. The variation of the width (g) of the channel of DGS resonator, while keeping all other dimensions constant, leads to a shifting of the resonance frequency along of frequency range, while the cutoff frequency remains invariable (see Fig. 13(a)). In other words, the variation of value of gap (g) from 0.5 mm to 2.5 mm leads to a variation of the attenuation pole frequency from 7 GHz to 9.5 GHz. The increase of the gap (g) causes a decrease of the DGS-capacitance and thus a shifting of the attenuation pole to the high frequency range.

In the second study, all other dimensions are maintained constant, while changing the length of the channel of the DGS unit. As Fig. 13(b) shows, the cutoff as well as resonance frequencies are changed

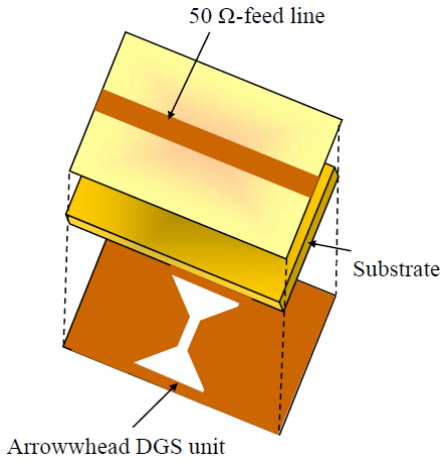

Figure 12. The 3D-view oft he DGS-element.

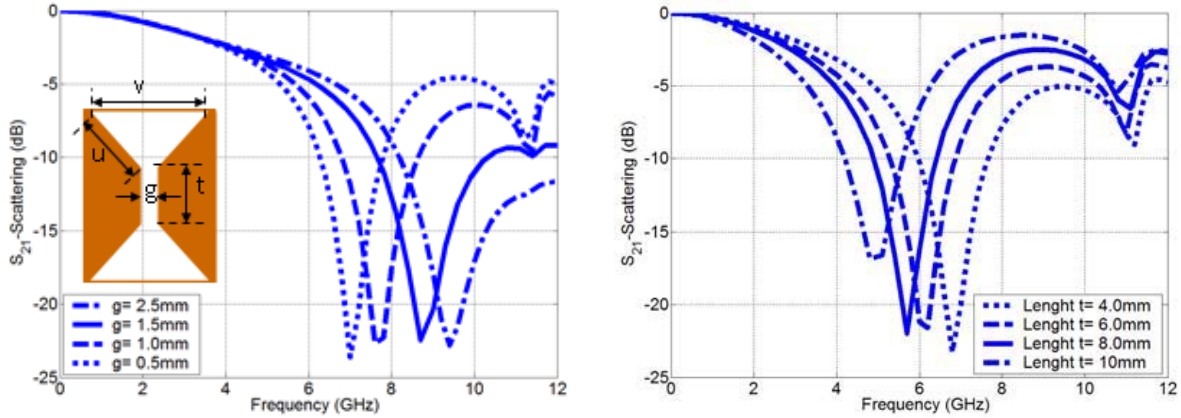

Figure 13. The S_{21} results: (a) versus DGS-gap (g), (b) versus DGS-length (t).

simultaneously. These characteristics can be useful for improvement of the rejects band of the low-pass filter. All the dimensions of the proposed arrowhead slot are depicted in Table 1.

7. PERFORMANCE ENHANCEMENT OF A LOW-PASS FILTER USING DGS AND OCTAGONAL RESONATORS

In order to show the improvement of features of the proposed low-pass filter, two octagonal microstrip resonators and one arrowhead DGS element are used. The DGS three-pole low-pass filter has been designed, optimized and simulated (see Fig. 14). The EM coupling between the two octagonal resonators and the DGS unit leads to an improvement of the stopband. In this work, the coupling distance (z) is chosen based on empirical method. The addition of DGS and thus a rise of slow wave effect regenerate a strong electromagnetic coupling between the DGS and both microstrip octagonal microstrip resonators, and this leads to a minimization of the loss in the passband and to a suppression of the undesired high harmonics of the stopband. The simulation results of this DGS LPF are obtained using Microwave Office as shown in Fig. 15. The substrate used is Rogers RO4003 with dielectric constant of 3.38, thickness of 0.813 mm, and dielectric loss tangent (δ) = 0.0027. Fig. 14 shows the 3D-view of the proposed DGS LPF. The topology has a cutoff frequency and resonance frequency at 2.4 GHz and 7 GHz, respectively. As depicted in Fig. 15, the simulated results show a wide rejection bandwidth with

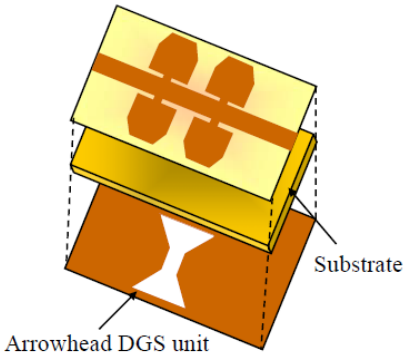

Figure 14. The layout of the DGS-octagonal LPF structure.

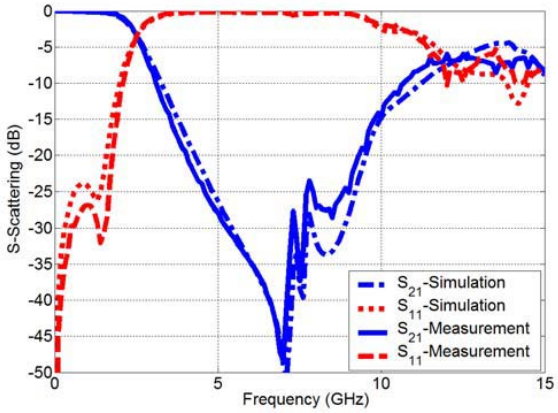

Figure 15. The scattering parameters of the DGSoctagonal LPF.

overall 20 dB attenuation from 4 GHz up to 9.5 GHz. The insertion loss is lower as 0.3 dB which leads to a deep return loss (greater than −25 dB). The comparison between measured and simulated results is depicted in Fig. 15. The simulated results agree closely with the measured ones. The dimensions of the LPF and the developed LPF are listed in Table 1.

8. DESIGN AND OPTIMISATION OF THE PROPOSED DGS-DMS LOW-PASS FILTER

In order to eliminate the undesired harmonics responses in the reject band, thus to improve the stopband and passband, a new 2.4 GHz DGS-DMS LPF combination is designed, optimized, simulated and fabricated. The DGS and DMS topologies are chosen in such a way that they operate around undesired frequency values, which present the resonance frequencies of harmonic responses, in our case around $4f_c$. This suppression leads to a compact structure with a broad reject band. As shown in Fig. 16, the proposed structure consists of two coupled octagonal microstrip resonators placed between two identically DMS units, which are electrically coupled through a substrate with a DGS shape. The last one is etched in the ground plane. The coupled distance ($z = 6$ mm) between the cascaded octagonal resonators is obtained based on empirical method. This proposed geometrical idea is realized using multilayer technique. The new filter-topology is simulated on a Rogers RO4003 substrate with a relative dielectric constant ε_r of 3.38 and thickness h of 0.813 mm. The proposed filter is designed to operate at a

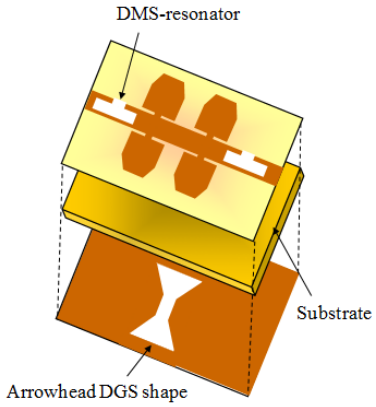

Figure 16. The 3D-view of the proposed DGS-DMS octagonal LPF structure.

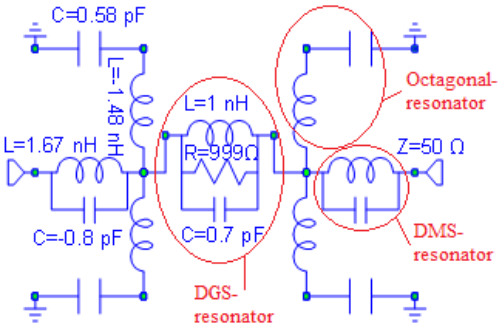

Figure 17. The equivalent circuit approach of the proposed DGS-DMS octagonal LPF structure.

cutoff frequency of 2.4 GHz. The simulation results show an insertion loss in the passband about 0.3 dB and an attenuation pole at 3.7 GHz. As described in Fig. 18, the simulation results show two reflection poles at 1.04 and 2 GHz with levels over 28 and 23 dB, respectively, and a transmission zero is located at 7.2 GHz with an attenuation level over 55 dB. The suppression of the undesired harmonics leads to an extended stopband with attenuation level better than 20 dB from 3.7 GHz to 9.5 GHz. Fig. 17 shows an equivalent circuit approach of the LPF. The DMS, DGS as well as the octagonal shapes are modeled by different parallel L-C circuits connected in series with a 50 Ω feed line. Until 8 GHz, the full-wave EM and circuit simulations agree well with each other. Beyond 8 GHz, a clear discrepancy is observed between the two results, and this disadvantage is due to the periodicity and thus to electrical behaviour of the designed filter topology.

Adding the capacitance and inductance using DGS and DMS, return loss in the stopband region is close to 0 dB, which shows a low radiation loss, and in parallel the insertion loss along the passband domain is close to 0 dB too.

In order to prove the effectiveness of proposed filter-idea, the structure is designed and simulated using emGine software while retaining the same conditions and features that have been used with AWR software. Fig. 19 shows the simulation results from DC to 10 GHz. The two simulations (Fig. 18 and Fig. 19) agree well with each other until 9 GHz. The two simulation results show a transmission zero at 7 GHz and cutoff frequency at 2.4 GHz. Because the measurements are similar to the simulations carried out by emGine software, we have decided to further optimize the EM-simulation results and to present in this work the figure, which compares the measured results and improved simulated results obtained using emGine-simulator (see Fig. 22).

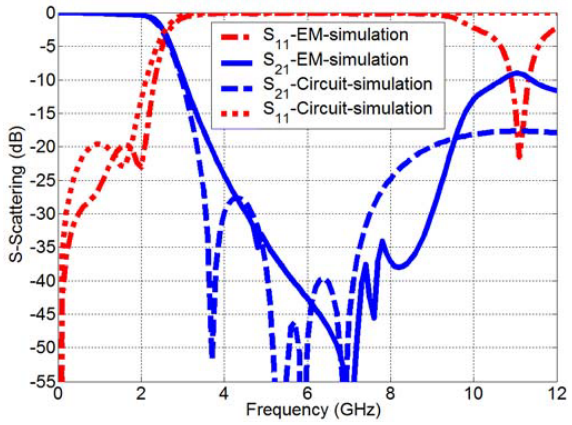

Figure 18. Comparison between simulation and circuit results of the proposed DGS-DMS octagonal LPF.

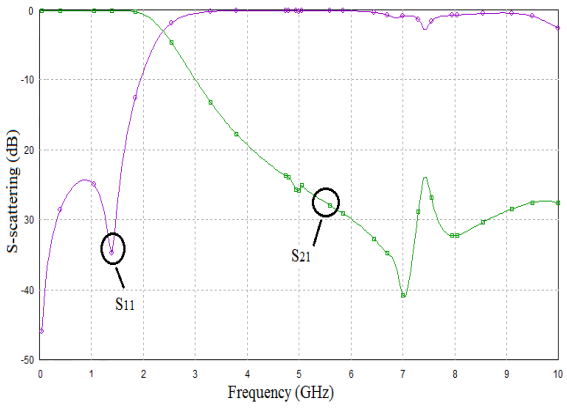

Figure 19. The simulation results of the proposed DGS-DMS octagonal LPF using emGine-simulator.

9. EM FIELD DISTRIBUTION OF THE PROPOSED FILTER TOPOLOGY

In order to find a relationship between the EM-simulation results and EM-field behaviour, an investigation of the surface electric and magnetic energies of proposed LPF structure is carried out as shown in Figs. 20(a) and (b). Two different frequency situations have been observed. At frequency 3 GHz, the full power is transmitted through the 50 Ω microstrip feed and DGS resonators from port 1 to port 2. The magnetic energy appears around the thin microstrip and near DGS patches (heads), while an equal amount of electric energy appears in the close gap of the DGS and between the two arms of DMS resonators. The structure is located then in the passband state. This field distribution shows that the metal areas around the DGS and DMS have inductance behavior while the gaps present capacitance behavior as shown in Fig. 20(a). At 7 GHz, almost the whole energy remains locked near the input of the structure and around the first DMS resonator. This behavior indicates that the low-pass filter is in the stopband state, as shown in Fig. 20(b).

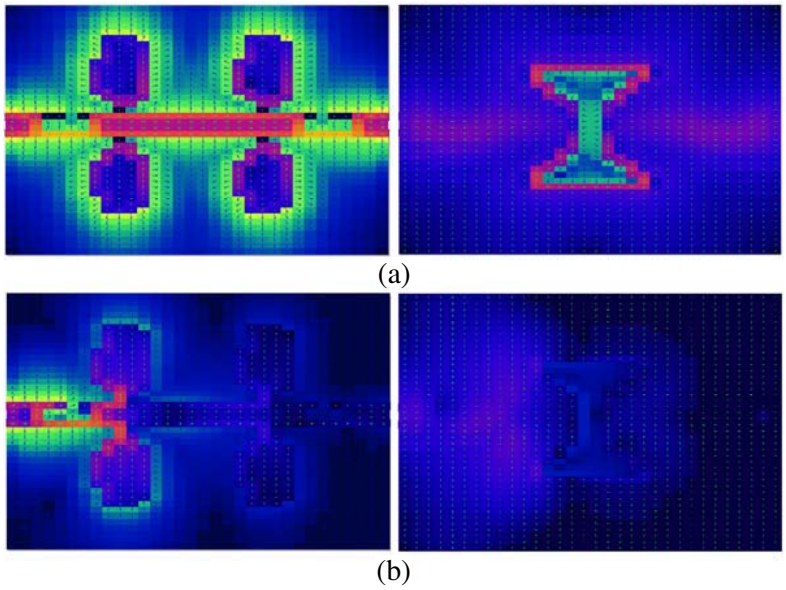

Figure 20. EM field distribution results: (a) in the passband at 1.5 GHz and (b) in the stopband at 7 GHz.

Finally, it can be confirmed that the DGS shape and the DMS resonator present two different equivalent LC-circuits. This EM-distribution approach helps to find a compromise between the physical principle and the behavior of DGS-DMS filter topology.

10. FABRICATION AND MEASUREMENTS OF THE DGS-DMS-LPF

The proposed filter is designed and fabricated on a substrate with relative permittivity of 3.38 and thickness (h) of 0.813 mm. The simulation is accomplished using AWR microwave office software and fabricated using photolithographic process. Fig. 21 shows photographs of the fabricated microstrip LPF with compact size of $30 \times 18\,\text{mm}^2$. The measurements are carried out on an HP8719D network analyzer. The comparison between the simulated and measured results is shown in Fig. 22. A very good agreement between simulations and measurements is obtained, and it confirms the validity of the DMS-DGS configuration and design procedure. The measured cutoff frequency (f_c) is 2.4 GHz with no more than 0.3 dB ripple level in the passband. The stopband attenuation is better than 20 dB from 3.42 to 12 GHz, and the return loss is less than 23 dB in the passband and close to 3.2 dB at the end of the stopband. A spurious harmonic suppression is achieved up to $5f_c$. The experimental results show good

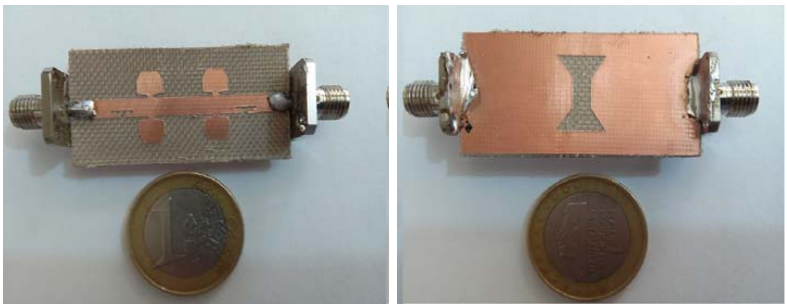

Figure 21. Photograph of the fabricated of the proposed DGS-DMS LPF: (a) top view, (b) bottom view.

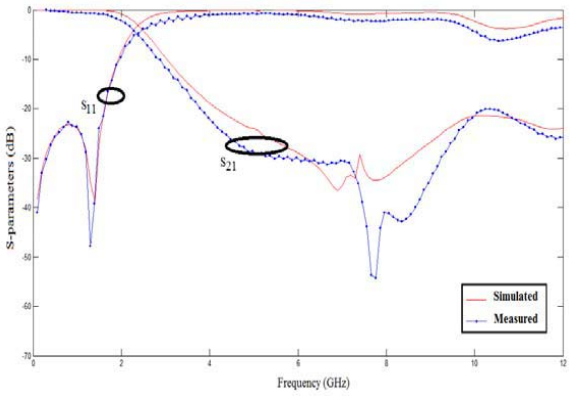

Figure 22. Comparison of the simulation and measurement results of the proposed DGS-DMS LPF.

agreement with the simulated ones in the performance of both insertion loss and return loss. The small deviations between the simulated and measured results can be interpreted as unexpected fabrication tolerances, SMA connectors, and manufacturing tolerance errors.

The sharpness factor and roll-off rate of the proposed LPF can be calculated as follows:

$$\mathrm{SF}(sharpness\,factor) = \frac{f_c}{f_0} \tag{6}$$

$$\xi(selectivity) = \frac{\alpha_{\min} - \alpha_{\max}}{f_s - f_c}\,(\mathrm{dB/GHz}) \tag{7}$$

where f_c, f_s, f_0, α and $\alpha_{\min}$ are the 3 dB cutoff frequency, attenuation pole frequency, first transmission zero, 3 dB attenuation point, and attenuation point at f_s (first attenuation pole), respectively. The sharpness factor and roll-off rate of the proposed filter reach SF = 0.51 and $\xi = 19$ dB/GHz successively. The performance comparison of the proposed low-pass filter with some other low-pass filters is shown in Table 2. It is clear from Table 2 that the proposed compact DMS-DGS microstrip low-pass filter offers a much wider rejection level of better than 20 dB from 3.42 to 12 GHz. It can be seen from Table 2 that the proposed filter provides good performances in stopband rejection and passband return loss and is smaller in size ($30 \times 18\,\mathrm{mm}^2$) than those reported in the literature.

Table 2. Comparison of the proposed DMS-DGS LPF with other related LPFs.

Ref.	Size (mm^2)	f_c (GHz)	Pass band Return loss (dB)	Stop band (GHz @dB)	Substrate dielectric constant/ height (mm)
[4]	35×71	0.5	16.3	0.5-4.5@20 dB	4.3/1.58
[6]	30×20	1.0	13.5	1.5−4.2@20dB	2.17/0.78
[10]	25×40	4.5	20	5.2−10@32dB	3.2/0.787
[11]	30×22	1.78	10.67	1.86−10.7@10dB	2.2/0.508
[13]	30×20	1.1	17	1.5−8.3 GHz@20dB	3.38/0.813
[15]	70×20	2.0	15	2.6−7 GHz@20dB	3.38/0.813
[17]	33×30	2.95	15	3.5-8.8@20dB	2.2/0.787
[18]	71×13	2.43	20	3.26-10@2dB	3.38/1.524
Proposed	30×18	2.0	29	3.42−12 GHz@20dB	3.38/0.813

11. IMPROVEMENT OF THE STOPBAND OF THE LPF USING TWO PARASITICS DGS SHAPES

One of the most important features of the low-pass filter is the stopband. In order to improve the reject band of our filter, it is necessary to suppress several harmonics of the high frequency range. To reach these aims two additional small DGSs are etched in ground plane and placed at the left and right of the arrowhead DGS resonator. The parasitic DGS element is chosen having a high resonance frequency. The value of the resonance frequency depends on dimensions of the DGS shape. Based on this characteristic, it is simple to use the DGS with desired resonance frequency in order to suppress the unwanted harmonics. Fig. 23 shows the 3D-view of the improved low-pass filter. The improved filter is designed and optimized on a substrate with the same parameters as before. The simulation process is accomplished using AWR microwave office software. As depicted in Fig. 24, the simulation results confirm the validity of the parasitic-DGS technique. The insertion loss from DC to 3 GHz is less than 0.3 dB, and the return loss is less than −22 dB in the passband. The stopband rejection levels are larger than 20 dB from 3.5 GHz to 17 GHz. The proposed filter exhibits sharp cutoff dropping from less than −0.5 dB to almost −44 dB within a range of 2 GHz. The size of the proposed band-stop filter is $30 \times 18\,\text{mm}^2$.

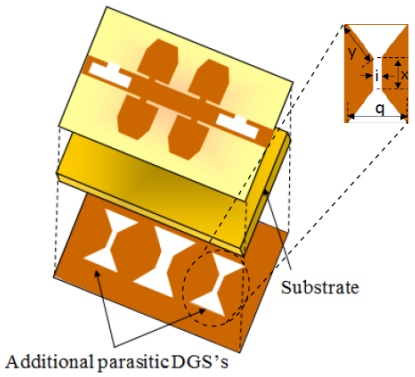

Figure 23. 3D-view of the improved LPF.

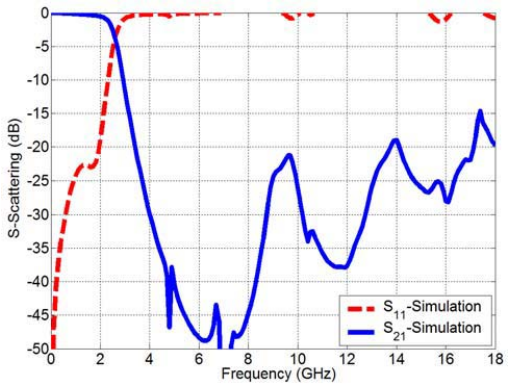

Figure 24. Simulated S-parameters of the improved LPF.

12. CONCLUSION

In this paper, a new compact low-pass filter (LPF) using a DGS-DMS combination and quasi octagonal resonator is introduced. The improved frequency response in the passband and stopband. The low-pass filter based on the proposed topology offers significant improvement of stopband, high harmonic suppressions, miniaturization, and a sharp cutoff frequency response. The investigated low-pass filter has a rejection level better than 20 dB from 3.42 to 12 GHz. The good agreement between the simulated and experimental results validates the proposed design. Moreover, the compact size is only $0.44\lambda_g \times 0.26\lambda_g \times 0.12\lambda_g$ with $\lambda_g = 68$ mm. The addition of two parasitics DGS elements in the ground plane leads to suppression of the undesired harmonics and thus to improvement the stopband while maintaining the same size of the previous filter structure. The features of proposed LPF such as planar configuration, low insertion loss, wide stopband, sharp roll-off, low cost, and compact structure with simple topology make the filter a promising candidate for applications in various mobile wireless communication systems as well as in microwave area such as L-band, GPS and RADAR.

ACKNOWLEDGMENT

The first author thanks the German Research Foundation (DFG) for financial support. The author thank M.Sc. Eng. Sonja Boutejdar, Mehdi Boutejdar, Karim Boutjdir, Mohamed Boutejdar, Larbi Boutjder for their assistance and University of Boumerdes, Institute of Electrical Engineers and Electronics (IGEE, Ex. INELEC), Dept. of Electronics, Boumerdes, Algeria for its help in fabrication.

REFERENCES

1. Auob, A. and L. Ali, "Compact lowpass filter with wide stop-band using open stubs loaded spiral microstrip resonant cell," *Aces Journal*, Vol. 16, 27–34, Jan. 2013.
2. Li, L. and Z.-F. Li, "Compact quasi-elliptic low pass filter using symmetric rectangular coupled capacitors," *Electron. Lett.*, Vol. 44, No. 2, 124–125, Jan. 2008.
3. He, Q. and C. Liu, "A novel low-pass filter with an embedded band-stop structure for improved stop-band characteristics," *IEEE Microw. Wireless Compon. Lett.*, Vol. 19, No. 10, 629–631, Oct. 2009.
4. Raphika, P. M., P. Abdulla, and P. M. Jasmine, "Compact low pass filter with a sharp roll-off using patch resonators," *Microwave and Optical Technology Letters*, Vol. 56, No. 11, 2534–2536, 2014.
5. Velidi, V. and S. Sanyal, "Sharp roll-off low pass filter with wide stopband using stub-loaded coupled line hairpin unit," *IEEE Microw. Wireless Compon. Lett.*, Vol. 21, No. 6, 301–303, 2011.
6. Chen, X., L. Zhang, Y. Peng, Y. Leng, H. Lu, and Z. Zheng, "Compact lowpass filter with wide stop band bandwidth," *Microwave and Optical Technology Letters*, Vol. 57, No. 2, 367–371, 2015.
7. Packiaraj, D., K. J. Vinoy, M. Ramesh, and A. T. Kalghatgi, "Design of compact low pass filter with wide stop band using tri-section stepped impedance resonator," *Int. J. Electron. Commun. (AEÜ)*, Vol. 65, 1012–1014, 2011.
8. Wang, L., H.-C. Yang, and Y. Li, "Design of compact microstrip low-pass filter with ultra-wide stopband using SIRs," *Progress In Electromagnetics Research Letters*, Vol. 18, 179–186, 2010.
9. Cao, H., W. Guan, S. He, and L. Yang, "Compact lowpass filter with high selectivity using G-shaped defected microstrip structure," *Progress In Electromagnetics Research Letters*, Vol. 33, 55–62, 2012.
10. Boutejdar, A., A. Elsherbini, and A. S. Omar, "A compact microstrip multi-layer lowpass filter using triangle slots etched in the ground plane," *36th European Microwave Conference, 2006*, 271–274, 2006.
11. Balalem, A., A. R. Ali, J. Machac, and A. Omar, "Quasi-elliptic microstrip low-pass filters using an interdigital DGS slot," *IEEE Microw. Wireless Compon. Lett.*, Vol. 17, No. 8, 586–588, Aug. 2007.
12. Chen, X.-Q., R. Li, S.-J. Shi, Q. Wang, L. Xu, and X.-W. Shi, "A novel low pass filter using elliptic shape defected ground structure," *Progress In Electromagnetics Research B*, Vol. 9, 117–126, 2008.
13. Hayati, M. and A. Lotfi, "Elliptic function low pass filter with sharp cutoff frequency using slit loaded tapered compact microstrip resonator cell," *IET Electronics Letters*, Vol. 46, No. 2, 143–144, 2010.
14. Boutejdar, A. and W. A. E. Ali, "Improvement of compactness of low pass filter using new Quasi-Yagi-DGS-resonator and multilayer-technique," *Progress In Electromagnetics Research C*, Vol. 69, 115–124, 2016.
15. Boutejdar, A., A. A. Ibrahim, and E. P. Burte, "Design of a novel ultra wide stop band low pass filter using a DMS-DGS technique for radar applications," *International Journal of Microwave Science and Technology*, 1–7, 2015.
16. Boutejdar, A., M. Makkey, A. Elsherbini, and A. Omar, "Design of compact stop band extended microstrip low pass filters by employing mutual coupled square-shaped defected ground structures," *Microwave and Optical Technology Letters*, Vol. 50, 1107–1111, 2008.
17. Boutejdar, A., A. Ramadan, M. Makkey, and A. S. Omar, "Design of compact microstrip low pass filters using a U-shaped defected ground structure and compensated microstrip Line," *Proceedings of the 36th European Microwave Conference*, 267–270, Manchester, UK, Sep. 2006.
18. Boutejdar, A., A. Elsherbini, and A. S. Omar, "Method for widening the reject-band in low-pass/band-pass filters by employing coupled C-shaped defected ground structure," *IET Microw. Antennas Propag.*, Vol. 2, No. 8, 759–765, 2008.
19. Mohra, A. S. S., "Compact lowpass filter with sharp transition band based on defected ground structures," *Progress In Electromagnetics Research Letters*, Vol. 8, 83–92, 2009.
20. Boutejdar, A, "Design of compact reconfigurable broadband band-stop filter based on a low-pass filter using half circle DGS resonator and multi-layer technique," *Progress In Electromagnetics Research C*, Vol. 71, 91–100, 2017.

21. Boutejdar, A., et al., "Design of a novel ultrawide stopband lowpass filter using a DMS-DGS technique for radar applications," *International Journal of Microwave Science and Technology*, Vol. 6, 1–7, 2015.
22. Challal, M., A. Boutejdar, M. Dehmas, A. Azrar, and A. Omar, "Compact microstrip low-pass filter design with ultra-wide reject band using a novel quarter-circle DGS shape," *Appl. Comp. Electro. Society (ACES) Journal*, Vol. 27, No. 10, 808–815, Oct. 2012.
23. Boutejdar, A., A. Omar, and E. Burte, "LPF builds on Quasi-Yagi DGS," *Microwaves & RF*, Vol. 52, 72–77, 2013.
24. Ting, S. W., K. W. Tam, and R. P. Martins, "Miniaturized microstrip low pass filter with wide stop-band using double equilateral U-shaped defected ground structure," *IEEE Microw. Wireless Compon. Lett.*, Vol. 16, 240–242, May 2006.
25. Boutejdar, A., "Design of a very compact U-HI-LO low-pass filter using meander technique and quasi horn inductors for L-band and C-band applications," *Microwave and Optical Technology Letters*, Vol. 58, No. 12, 2897–290, 2016.
26. Peng, L., et al., "A low-pass filter with sharp transition and wide stop-band designed based on new metamaterial transmission line," *Applied Computational Electromagnetics Society Journal*, Vol. 31, No. 10, 1250–1256, 2016.